ELSEVIER

Catalysis Today 52 (1999) 279–289

CATALYSIS TODAY

www.elsevier.com/locate/cattod

Modelling of a bubble column slurry reactor for Fischer–Tropsch synthesis

C. Maretto[a,*], R. Krishna[b,1]

[a]*Advanced Engineering, EniTecnologie S.p.A., S. Donato Milanese (MI), Italy*
[b]*Department of Chemical Engineering, University of Amsterdam, Amsterdam, Netherlands*

Abstract

This work deals with the simulation of a commercial size slurry bubble column reactor for catalytic conversion of syngas ($CO+H_2$) to liquid hydrocarbons (Fischer–Tropsch synthesis). The reactor was assumed to operate in the heterogeneous or churn-turbulent flow regime and the complex hydrodynamics of the slurry bubble column was described by means of a model, based on an extended experimental program, which takes into account the effect of column diameter, slurry concentration, system properties and pressure on the gas holdup. The reactor model was developed adopting two different classes of bubbles: large bubbles (20–70 mm) which rise through the column virtually in plug-flow, and small bubbles (1–10 mm) which are entrained in the slurry phase (liquid+solid catalyst particles). The slurry phase, together with the entrained small bubbles, was considered completely mixed due to the upward motion of the fast-rising large bubbles. The reaction kinetics was chosen from the literature and referred to a cobalt based catalyst. Design calculations have been carried out for a plant with a 5000 t/day capacity for producing middle distillates. Operating conditions with respect to superficial gas velocity and slurry concentration are suggested so as to achieve the optimum reactor performance.

Keywords: Bubble column; Slurry reactor; Heterogeneous regime; Natural gas conversion; Liquid fuels; Fischer–Tropsch synthesis

1. Introduction

There is a need from the natural gas and energy industries to seek for an economically attractive way of converting remote gas reserves into transportable products, such as high quality fuels or petrochemicals. A possible way for the conversion of natural gas to middle distillates is based on a three-step process. Firstly, production of syngas from natural gas (catalytic partial oxidation, steam reforming or autothermal reforming). Secondly, catalytic conversion of syngas into hydrocarbons, mostly paraffins from C_5 to C_{100+} (Fischer–Tropsch (F–T) synthesis). Thirdly, hydrocracking of the heavy paraffinic hydrocarbons to middle distillates. The F–T synthesis step is highly exothermic. In order to control the temperature within the reactor, when considering high capacity plants (e.g. 5000 t/day of middle distillates), the bubble column slurry reactor is the preferred choice when compared to a fixed bed reactor [1,2], because of the possibility in the slurry type reactor to achieve almost isothermal conditions (heat transfer coefficient on the slurry side is much higher compared to that of a fixed bed).

*Corresponding author. Tel.: +39-2-52046443; fax: +39-2-52036116.

[1]Tel.: +31-20-5257007; fax: +31-20-52555604

E-mail address: cmaretto@enitechnologie.eni.it (C. Maretto)

0920-5861/99/$ – see front matter
PII: S0920-5861(99)00082-6

Slurry bubble column hydrodynamics is very complex and significantly influenced by the size of the column. Hence, it becomes essential to study the influence of scale on relatively large cold-flow experimental equipment, in order to predict the hydrodynamic parameters for industrial size bubble column reactors (5–8 m diameter). Scale-up information on slurry bubble column hydrodynamics was obtained by means of an extensive experimental program carried out at the University of Amsterdam [3–7]. Different liquids (water, paraffin oil, ethanol and tetradecane) and slurries of paraffin oil and silica particles at concentrations up to 37% in volume were used in columns of 0.05, 0.10, 0.174, 0.19, 0.38 and 0.63 m diameter. The silica particles used had a size distribution, d_p: 10%<27 μm; 50%<38 μm; 90%<47 μm.

The hydrodynamic model resulting from these studies was used to develop a model for performing slurry reactor design and optimisation, applied to the Fischer–Tropsch synthesis process. As regards F–T kinetics, which is scale independent, a reaction scheme from published literature [8] was chosen. Simulations of the slurry reactor were carried out in order to study the influence of the inlet superficial gas velocity and the catalyst loading on conversion, reactor productivity and the number of internal cooling tubes. A sensitivity analysis was also carried out to check the dependence of the reactor productivity on mass transfer and kinetic parameters.

2. Catalysis and reaction kinetics

The Fischer–Tropsch synthesis can be described by the following, simple reaction:

$$CO + 2H_2 \rightarrow -(CH_2)- + H_2O$$

where –(CH_2)– is the methylene group, which polymerises into a hydrocarbon chain. Water, formed as primary product can react with CO to form CO_2, as a side reaction:

$$H_2O + CO \leftrightarrow CO_2 + H_2 \text{ (water gas shift)}$$

Commonly used catalysts for F–T synthesis are based on supported iron or cobalt, with or without the presence of other metals as promoters (e.g. Cu, Mn, Zr, K, Na, Sc, Mo, W, Ru, Ti, Re, etc.). The catalyst support can be titania (TiO_2), silica (SiO_2) or alumina (Al_2O_3). The effect of promoters is to increase reaction rate and selectivity to heavy hydrocarbons and to reduce catalyst deactivation. Iron based catalysts are cheap and exhibit a high selectivity to olefins and light hydrocarbons. They are active with respect to water gas shift function and produce large amounts of oxygenates. However, iron catalyst deactivates rapidly due to coke deposition on catalyst surface and oxidative reactions. Cobalt based catalysts generate higher molecular weight hydrocarbons (paraffinic waxes) and promote hydrogenation. They deactivate much less in comparison with iron catalysts and produce limited amounts of oxygenates. Generally speaking, the water gas shift activity of cobalt catalyst is negligible. The above mentioned characteristics make the cobalt based catalysts the more attractive ones for natural gas conversion to middle distillates.

The intrinsic kinetic equation for the consumption rate of syngas, chosen in the literature, was that proposed by Yates and Satterfield [8], which is a Langmuir–Hinshelwood type

$$-R_{CO+H_2} = \frac{a \cdot p_{H_2} \cdot p_{CO}}{(1 + b \cdot p_{CO})^2}. \quad (1)$$

The rate of the synthesis gas consumption was measured in a continuous, mechanically stirred, 1 l slurry autoclave. The catalyst was Co/MgO on SiO_2 support. The range of operating conditions used were: 220–240°C, 5–15 bar, 1.5–3.5 as H_2/CO feed ratios. The achieved H_2 and CO conversions ranged between 6–68% and 11–73% respectively. The kinetic constant, a, and the absorption coefficient of species CO, b, were determined by means of non-linear fit of experimental data

$$a = 8.8533 \times 10^3 \cdot \exp\left[4494.41\left(\frac{1}{493.15} - \frac{1}{T}\right)\right] \text{ mol}/(\text{s kg}_{\text{cat}} \text{ bar}^2), \quad (2)$$

$$b = 2.226 \cdot \exp\left[-8236\left(\frac{1}{493.15} - \frac{1}{T}\right)\right] \text{ 1/bar}. \quad (3)$$

A simpler first-order kinetics, like the one proposed by Post et al. [9] for a zirconium-promoted cobalt catalyst on silica support

$$-R_{CO} = k p_{H_2}, \quad (4)$$

has been incorporated in various other reactor models for F–T synthesis slurry bubble column reactors [10]. However, the Yates–Satterfield kinetics is more realistic than that of Post et al. [9], when operating at high syngas conversion (above 60%) and when the H_2/CO feed ratio is close to the stoichiometric ratio (i.e. when H_2 is not the limiting species). For cobalt catalyst with negligible water gas shift activity the H_2/CO stoichiometric ratio is nearly 2.

To describe catalyst selectivity, the Anderson–Schultz–Flory mechanism for the carbon atom distribution was chosen. Considering that most of the hydrocarbon products are paraffins, the molar fraction of each species C_nH_{2n+2}, is defined as follows:

$$x_n = (1 - \alpha_{ASF})\alpha_{ASF}^{n-1}, \quad (5)$$

where α_{ASF} is the Anderson–Shultz–Flory coefficient, that is the probability factor of hydrocarbon chain growth. The higher the α_{ASF} coefficient, the higher the fraction of heavy paraffins. A value of α_{ASF}=0.9 was chosen [11].

3. Hydrodynamics of slurry bubble column reactor

Slurry bubble column reactors can operate either in the homogeneous flow regime or in heterogeneous (churn-turbulent) flow regime. Homogeneous regime is established within the reactor, when operating at low gas flow rates: small bubbles of gas (1–10 mm) are uniformly distributed into the slurry phase (liquid+ solid catalyst). With increasing gas throughput, transition from homogeneous to churn-turbulent regime occurs. In the heterogeneous regime small bubbles combine in clusters to form large bubbles (20–70 mm). These large bubbles travel up through the column at high velocities (in the range 1–2 m/s), in a more or less plug-flow manner. These large bubbles have the effect of churning up the slurry phase. Small bubbles, which co-exist with large bubbles in the churn-turbulent regime, are "entrained" in the slurry phase and as a good approximation have the same backmixing characteristics of the slurry phase. The hydrodynamics of a slurry bubble column reactor operating in the churn-turbulent regime is pictured in Fig. 1.

The churn-turbulent regime of operation is the most optimal one for F–T synthesis [1]. One of the most important parameters to be estimated for slurry reactor design and scale-up is the holdup of gas bubbles in the reactor, ϵ. Following the model of Krishna et al. [4] for churn-turbulent regime, the gas holdup can be determined as follows:

$$\epsilon = \epsilon_b + \epsilon_{df}(1 - \epsilon_b) \quad (6)$$

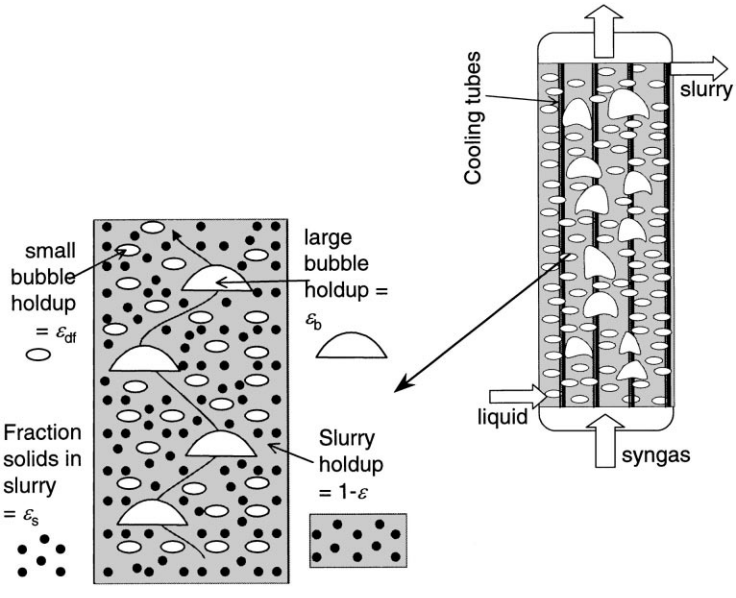

Fig. 1. Hydrodynamic picture of a bubble column slurry reactor operating in the churn-turbulent regime.

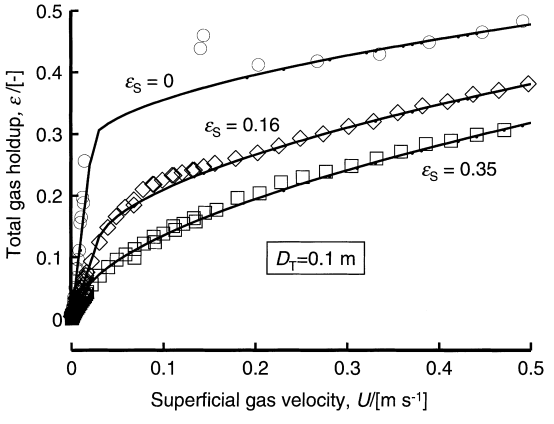

Fig. 2. Influence of increased slurry concentration, ϵ_s, on total gas holdup.

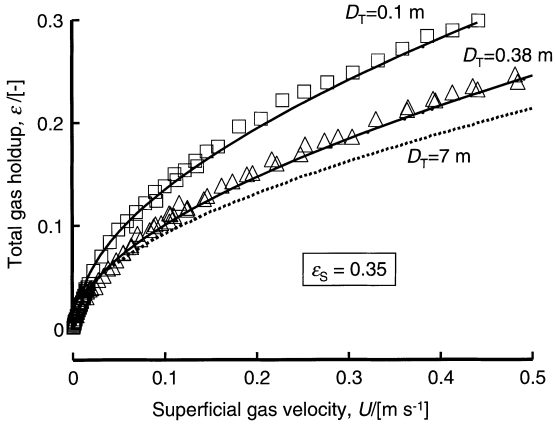

Fig. 3. Influence of increased column diameter on total gas holdup.

with ϵ_b the large bubble holdup and ϵ_{df} the small bubble holdup. Even though in reality the bubble population in the churn-turbulent regime has a broad size distribution, our chosen model considers only two bubble classes (large and small), whose characteristics have been mentioned in the foregoing paragraph. Small bubble holdup, ϵ_{df}, in the churn-turbulent regime, remains roughly constant when increasing superficial gas velocity. ϵ_{df} is set equal to the value of gas holdup at the regime transition point. The gas holdup in the reactor is affected by catalyst concentration, column diameter and pressure.

The effect of catalyst concentration, defined here as volume fraction in the slurry phase, ϵ_s (gas-free basis), is very strong, as it can be seen in Fig. 2 [5]. Addition of solid particles enhances coalescence of small bubbles, increasing the range of small bubble size and decreasing their holdup, and consequently the total gas holdup. The correlation for small bubble holdup, obtained by experimental data fitting [5], is the following:

$$\epsilon_{df} = \epsilon_{df,ref}\left(1 - \frac{0.7}{\epsilon_{df,ref}} \cdot \epsilon_s\right), \tag{7}$$

where $\epsilon_{df,ref}$ is the small bubble holdup in pure liquid (without solid). In the calculations of ϵ_s, it is assumed that the catalyst particle pores are completely filled by liquid. Eq. (7) shows that the small bubble holdup decreases with increasing solids volume fraction ϵ_s; at a solids holdup ϵ_s of about 38% the small bubble population is virtually destroyed and only large bubbles are present within the slurry bubble column reactor. A further assumption of our model is that the holdup of large bubbles is not influenced by catalyst concentration.

The increase in small bubble size due to increased catalyst concentration causes an increase in their rise velocity, V_{small}:

$$V_{small} = V_{small,ref}\left(1 + \frac{0.8}{V_{small,ref}} \cdot \epsilon_s\right), \tag{8}$$

where $V_{small,ref}$ is the rise velocity of small bubbles in pure liquid. The parameters $\epsilon_{df,ref}$ and $V_{small,ref}$ must be determined experimentally, and depend on the liquid properties. For paraffin oil $\epsilon_{df,ref}$=0.27 and $V_{small,ref}$=0.095 m/s, as determined during cold-flow experiments [5]. These model parameter values, along with Eqs. (7) and (8), determined on the basis of cold-flow experimental studies with paraffin oil slurries [5], are expected to hold also for the F–T slurry system.

The influence of column diameter on total gas holdup is illustrated in Fig. 3, where data for 0.1 and 0.38 m columns, at 35 vol% slurry, are compared. Column diameter influences large bubbles rise velocity; increasing the diameter of the reactor increases the rise velocity of large bubbles, therefore decreases large bubble holdup, and, as a consequence, decreases the total gas holdup. The large bubble holdup for

slurry concentrations ϵ_s above 0.16, can be estimated by the following relation [5]:

$$\epsilon_b = 0.3 \frac{1}{D_T^{0.18}} \frac{1}{(U - U_{df})^{0.22}} (U - U_{df})^{4/5}, \quad (9)$$

where D_T is the column diameter, U the overall superficial gas velocity, U_{df} the superficial velocity through the small bubbles, while $(U-U_{df})$ is the superficial velocity through the large bubbles (see Fig. 1). U_{df} is given by

$$U_{df} = \epsilon_{df} \cdot V_{small}. \quad (10)$$

This model assumes that column diameter dependence of large bubble holdup persists up to 1 m. For larger columns, such as industrial slurry reactors, D_T=1 has to be set into Eq. (9).

In Fig. 3 the total holdup curve for a 7 m column diameter, estimated by means of the hydrodynamic model [5] described by Eqs. (6)–(10), is presented. It should be evident from Fig. 3 that scaling-up from say 0.1 m diameter pilot plant to a 7 m diameter commercial scale reactor is not straightforward and careful attention has to be paid to scale-up rules.

Also pressure effects must be taken into account when scaling-up the results of cold-flow hydrodynamic studies. Such cold-flow hydrodynamic studies are usually performed at atmospheric pressure and room temperature, with air or nitrogen as gas phase; the gas density under these conditions is 1.3 kg/m^3. Commerical F–T synthesis is carried out under pressure (30–40 bar) and temperature (200–250°C for cobalt based catalysts). The density of syngas at 30 bar and 240°C is 7 kg/m^3. When pressure (or gas density) is increased, total gas holdup increases and transition from homogeneous to churn-turbulent regime is delayed [6]. The superficial gas velocity at the regime transition point shifts to higher values with increased system pressures. This implies that the gas holdup at the regime transition point increases with increasing system pressure; this effect is opposite to that of increasing solids concentration. The correlation of Reilly et al. [12], for small bubble holdup is recommended when no experimental data in pressure are available. This correlation predicts that the holdup of the small bubbles at the regime transition point, ϵ_{trans}, increases with $\rho_G^{0.48}$. The pressure effect is introduced in Eq. (7) as follows, keeping in mind that $\epsilon_{df} \approx \epsilon_{trans}$:

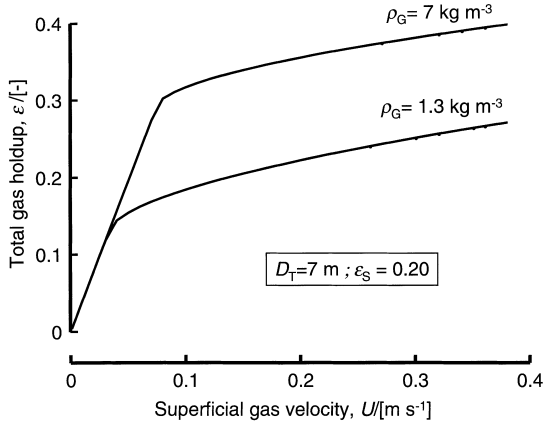

Fig. 4. Influence of increased gas density on total gas holdup.

$$\epsilon_{df} = \epsilon_{df,ref} \left(\frac{\rho_G}{\rho_{G,ref}} \right)^{0.48} \left(1 - \frac{0.7}{\epsilon_{df,ref}} \cdot \epsilon_s \right), \quad (11)$$

where $\rho_{G,ref}$ is the density of gas at ambient conditions. The strong influence of pressure on the total gas holdup is demonstrated in Fig. 4 for a 7 m diameter reactor, with a 20 vol% slurry. The volumetric mass transfer coefficient, k_La, is another important parameter, which has to be introduced in the reactor model. The most accepted correlations for k_La in the literature are those of Akita–Yoshida [13] and Calderbank–Moo-Young [14], but these correlations were obtained in bubble columns operating in the homogeneous regime and are able to describe only mass transfer from small bubbles, which are considered as rigid spheres.

Vermeer and Krishna [15] measured k_La from large bubbles, and found higher values of k_La, compared to those predicted by Akita's and Calderbank's correlations whether considering bubble sizes in the range 20–70 mm. Large bubbles continuously coalesce and break-up, while rising along the column, at a very high frequency (2–16 Hz) [7]. This is very important for interphase mass transfer, because the really large sized bubbles have only a momentary existence. Hence, gas–liquid interface renewal is very frequent and mass transfer characteristics of such large bubbles are better than those predicted by conventional theories.

The Vermeer–Krishna data for the N_2–turpentine-5 system, showed a constant value for the ratio between

$k_L a$ and the gas holdup of the large bubbles

$$\left(\frac{(k_L a)_{\text{large}}}{\epsilon_b}\right)_{N_2\text{-turpentine-5}} = 0.5\,\text{s}^{-1}. \tag{12}$$

The above ratio can be taken as a reference constant to predict $k_L a$ of large bubbles for different systems

$$\left(\frac{(k_L a)_{\text{large}}}{\epsilon_b}\right) = \left(\frac{(k_L a)_{\text{large}}}{\epsilon_b}\right)_{N_2\text{-turpentine-5}} \sqrt{\frac{D_L}{D_{L,\text{ref}}}} = 0.5\sqrt{\frac{D_L}{D_{L,\text{ref}}}}, \tag{13}$$

where D_L is the diffusion coefficient in the liquid phase, while $D_{L,\text{ref}}$ is equal to 2×10^{-9} m^2/s. The mass transfer coefficient for the small bubble population is determined in an analogous manner using a constant 1.0 in place of 0.5, i.e.

$$\frac{(k_L a)_{\text{small}}}{\epsilon_{df}} = 1.0\sqrt{\frac{D_L}{D_{L,\text{ref}}}}. \tag{14}$$

The diffusivities, D_L, of the H_2 and CO species at a reaction temperature of 240°C are 17.2×10^{-9} and 45.5×10^{-9} m^2/s, respectively.

4. Fischer–Tropsch slurry reactor model

The slurry reactor model was developed for a F–T industrial unit operating in the churn-turbulent regime at pressure 30 bar and temperature 240°C, with diameter D_T=7 m and dispersion height H=30 m. Large bubbles were assumed to be in plug-flow, passing through the column with a superficial gas velocity $U-U_{df}$. The liquid phase with the suspended catalyst and the entrained small bubbles are considered to be well mixed. These assumptions are consistent with the hydrodynamic studies [2–7] and the commercial reactor size. The conceptual reactor model is depicted in Fig. 5.

The model also assumes isothermal conditions within the reactor and catalyst particles, which have an average size of 50 μm, uniformly distributed within the slurry phase.

The mass balances which constitute the model are given below for:

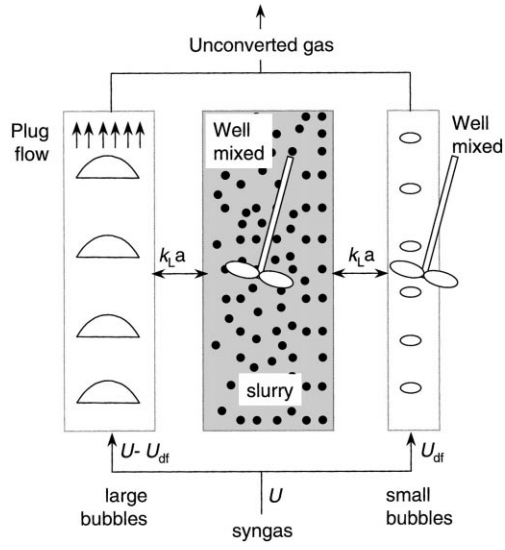

Fig. 5. Conceptual model of the Fischer–Tropsch slurry reactor.

(a) large bubbles:

$$-\frac{d}{dz}((U-U_{df})c_{G,CO\,\text{large}}) - (k_L a)_{CO,\text{large}}\left(\frac{c_{G,CO\,\text{large}}}{m_{CO}} - c_{L,CO}\right) = 0, \tag{15}$$

$$-\frac{d}{dz}((U-U_{df})c_{G,H_2\,\text{large}}) - (k_L a)_{H_2,\text{large}}\left(\frac{c_{G,H_2\,\text{large}}}{m_{H_2}} - c_{L,H_2}\right) = 0. \tag{16}$$

(b) small bubbles:

$$A\cdot U_{df}(c^{i}_{G,CO} - c_{G,CO\,\text{small}}) = (k_L a)_{CO,\text{small}}\left(\frac{c_{G,CO\,\text{small}}}{m_{CO}} - c_{L,CO}\right)AH, \tag{17}$$

$$A\cdot U_{df}(c^{i}_{G,H_2} - c_{G,H_2\,\text{small}}) = (k_L a)_{H_2,\text{small}}\left(\frac{c_{G,H_2\,\text{small}}}{m_{H_2}} - c_{L,H_2}\right)AH, \tag{18}$$

where it is assumed that at the reactor inlet: $c^{i}_{G,CO\,\text{small}} = c^{i}_{G,CO\,\text{large}} = c^{i}_{G,CO}$, and the same is true for hydrogen. Another assumption is that the gas velocity through small bubbles, U_{df}, remains constant along the reactor height.

(c) liquid phase:

$$A\int_0^H (k_La)_{CO,large}\left(\frac{c_{G,CO\,large}}{m_{CO}} - c_{L,CO}\right)dz + AH(k_La)_{CO,small}\left(\frac{c_{G,CO\,small}}{m_{CO}} - c_{L,CO}\right) + \cdots - AU_L^o c_{L,CO} - AH\epsilon_L \frac{a^* c_{L,CO} c_{L,H_2}}{(1+b^* c_{L,CO})^2} = 0, \quad (19)$$

$$A\int_0^H (k_La)_{H_2,large}\left(\frac{c_{G,H_2\,large}}{m_{H_2}} - c_{L,H_2}\right)dz + AH(k_La)_{H_2,small}\left(\frac{c_{G,H_2\,small}}{m_{H_2}} - c_{L,H_2}\right) + \cdots - AU_L^o c_{L,CO} - 2AH\epsilon_L \frac{a^* c_{L,CO} c_{L,H_2}}{(1+b^* c_{L,CO})^2} = 0. \quad (20)$$

ϵ_L is the slurry holdup, $\epsilon_L = 1-\epsilon$, where ϵ is the total gas holdup, estimated according to the hydrodynamic model summarised in Section 3. The parameters m_{CO} and m_{H_2} are the solubilities of CO and H_2 defined by $c_G = m \cdot c_L^*$. Estimated values of these solubilities in the paraffin $C_{16}H_{34}$ (taken as F–T liquid phase for properties evaluation), at a temperature of 240°C, are m_{CO}=2.478 and m_{H2}=2.964.

As the CO/H_2 feed ratio was set equal to the CO/H_2 consumption ratio (which is 2), the conversion of CO and H_2 are both equal to one another, and to the syngas conversion, χ_{CO+H_2}. In Eqs. (19) and (20) the kinetic equations are incorporated taking into account that $R_{H_2} = 2R_{CO}$.

The model considers that resistance to mass transfer between the liquid phase and the catalyst surface, and intraparticle diffusion resistance are negligible. A further simplification considers that the contraction of gas volume, due to synthesis gas conversion, affects only the large bubbles. The contraction factor α (for 100% syngas conversion) was calculated as $\alpha = -0.648$, assuming a 5 vol% of inert content in the syngas. The superficial gas velocity through large bubbles decreases with conversion according to the following relation:

$$U - U_{df} = (U^i - U_{df})(1 + \alpha\chi_{CO+H_2}). \quad (21)$$

The solution to the set of model equations represented by Eqs. (15)–(21) was implemented in a Fortran code. Since differential mass balances for the large bubbles are coupled with algebraic ones for the small bubbles and the liquid phase, the above system was solved by means of an iterative procedure. However, a simplification was possible, describing the concentration of one reactant as a function of the other one.

Since isothermal conditions are assumed within the reactor, the heat produced by the reaction ($\Delta H = -0.172$ MJ/mol_{CO}) must be completely removed. Vertical cooling tubes of 50 mm were installed in the reactor with coolant flow inside the tubes. The heat transfer coefficient from slurry to the coolant was estimated using the correlation of Deckwer et al. [16]:

$$St = 0.1 \cdot (Re \cdot Fr_G \cdot Pr^2). \quad (22)$$

The temperature difference between the reactor and the coolant was taken 10°C.

The slurry density is calculated from

$$\rho_{SL} = \rho_L\left(1 - \frac{\rho_L}{\rho_{SK}} \cdot \epsilon_s\right) + \rho_p \cdot \epsilon_s, \quad (23)$$

where ρ_p is the catalyst particle density (kg of solids/m^3 of particle including voids), while ρ_{SK} is the catalyst skeleton density (kg of solids/m^3 of solids without voids). The particles are assumed to be completely filled by liquid.

In order to determine the slurry viscosity, the modified Einstein's equation was taken in the calculations

$$\mu_{SL} = \mu_L(1 + 4.5 \cdot \epsilon_s). \quad (24)$$

5. Simulation results

The results of the simulations performed with the reactor model described above are presented here. The influence of the superficial gas velocity, U, and the catalyst concentration, ϵ_s, on synthesis gas conversion, total reactor productivity and number of internal cooling tubes were studied. A sensitivity analysis to check the influence of kinetics and mass transfer parameters was also carried out.

Simulations were carried out for a range of superficial gas velocities U=0.12–0.4 m/s, while the catalyst concentration range was ϵ_s=0.20–0.35.

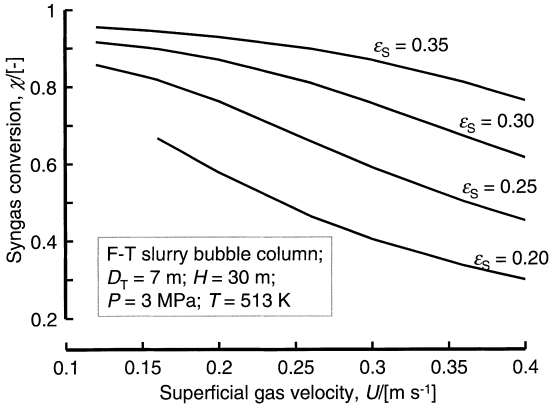

Fig. 6. F–T reactor simulation results: syngas conversion.

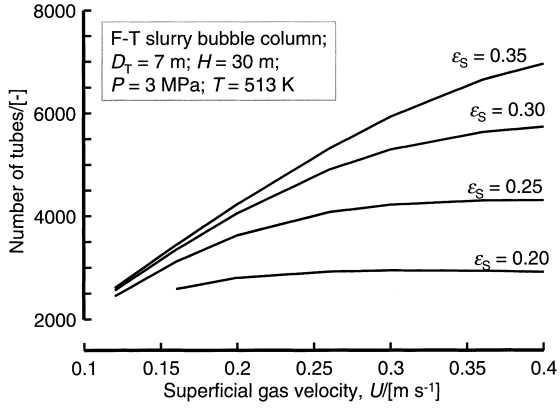

Fig. 8. F–T reactor simulation results: number of cooling tubes.

The main results of the simulations are reported in Figs. 6–8. In Table 1 operating conditions, liquid and catalyst properties used in the model are listed.

Increasing the inlet superficial gas velocity causes a decrease in conversion of the gas phase (Fig. 6), while reactor productivity increases (Fig. 7), and so does the number of tubes necessary to remove the heat produced by the synthesis reaction (Fig. 8). For example, for the case ϵ_s=0.30, while conversion changes from 96% at the lower gas velocity, to 63% at the higher, the productivity of the reactor increases from 1200 to 2640 t_{C1+}/day and the required number of cooling tubes increases from 2700 to 5900. In this case it is evident that, at the highest reactor productivity, the conversion of syngas is not complete, and the non-reacted syngas should be recycled to the reactor. In practice it is desirable to operate at conversion levels of about 90% per single pass avoiding the recycle of the gas phase. Therefore, it is necessary to operate at superficial gas velocities below 0.3 m/s (see Fig. 6).

Increasing catalyst concentration in the slurry phase, ϵ_s, increases both conversion and reactor productivity, as well as the number of internal cooling tubes to be installed in the reactor (see Figs. 6–8).

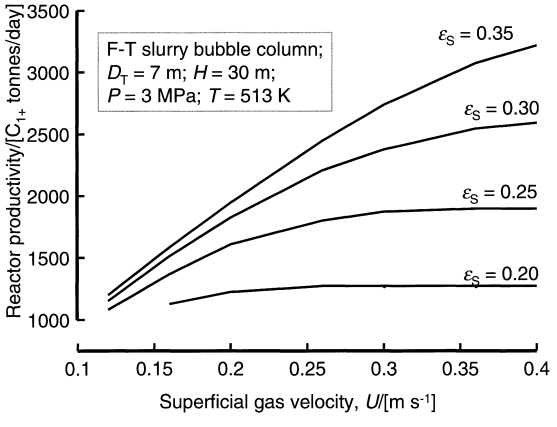

Fig. 7. F–T reactor simulation results: total reactor productivity.

Table 1
Operating conditions and system properties

Operating conditions	
Reactor temperature (T)	240°C
Reactor pressure (P)	30 bar
Reactor diameter (D_T)	7 m
Dispersion height (H)	30 m
Vertical cooling tube diameter (d_t)	50 mm
Vertical cooling tube height (H_t)	30 m
Temperature of coolant (T_w)	230°C
Liquid phase properties ($C_{16}H_{34}$)	
Density (ρ_L)	640 kg/m^3
Viscosity (μ_L)	2.9×10^{-4} Pa s
Surface tension (σ_L)	0.01 N/m
Thermal conductivity (λ_L)	0.113 W/m K
Heat capacity ($c_{p,L}$)	1500 J/kg K
Catalyst properties (silica support)	
Partial density (ρ_p)	647 kg/m^3
Pore volume (V_o)	0.00105 m^3/kg
Skeleton density (ρ_{SK})	2030 kg/m^3
Thermal conductivity (λ_s)	1.7 W/m K
Heat capacity ($c_{p,s}$)	992 J/kg K

The influence of ϵ_s is not only on the reaction kinetics, which is proportional to catalyst loading, but also on the total gas holdup. As already mentioned, increasing ϵ_s reduces gas holdup, ϵ; this means a higher slurry holdup, ϵ_L ($\epsilon_L=1-\epsilon$), i.e. more catalyst can be loaded within the reactor. Hence the increase of ϵ_s has more than a proportional effect on reactor performance.

As regards the pitch of the vertical cooling tubes, this varies between 12 and 19 cm, depending on the number of tubes required, according to simulation results. This pitch is considered large enough not to influence the hydrodynamics of the column, such as bubble size, bubble holdup or slurry phase backmixing.

A sensitivity analysis was also performed to study the influence of interphase mass transfer and kinetics on the reactor productivity. The superficial gas velocity was set $U=0.4$ m/s and the catalyst fraction $\epsilon_s=0.25$. A 10-fold increase or a 3-fold reduction of k_La with respect to the base case value, has a negligible effect on reactor productivity. On the other hand, increasing the Yates–Satterfield kinetic constant, a, by a factor 2, causes a 60% increase in the reactor productivity. Sensitivity with respect to reduced catalyst activity was not considered because all development efforts should be directed at improving catalyst formulations. Therefore, interphase mass transfer does not influence the reactor performance while the system is very sensitive to the kinetic term. Under the assumed conditions the process appears to be chemically controlled.

6. Conclusions

From simulation studies of a slurry bubble column reactor for Fischer–Tropsch synthesis operating in the churn-turbulent regime, the following conclusions can be reached:

(1) To obtain the best reactor performance, we must operate at the highest catalyst concentration compatible with slurry handleability (e.g. separation unit). From cold-flow experimental studies, carried out at the University of Amsterdam, the feeling is that $\epsilon_s=0.4$ is the maximum catalyst concentration in the slurry phase, which can be used in commercial practice.

(2) Assuming a conservative value for $\epsilon_s=0.35$, and an inlet superficial gas velocity $U^i=0.3$ m/s, three parallel reactors (7 m diameter$\times$30 m dispersion height) are required for an assigned capacity of 5000 t/day of middle distillates. It was assumed that middle distillate products are 70% of total reactor production rate. At the chosen operating conditions, the number of tubes to be installed per each reactor is 6000, and the pitch is 15 cm.

(3) If the catalyst activity were twice that of Yates–Satterfield, then the number of reactors in parallel necessary to produce 5000 t/day of middle distillates would reduce from 3 to 2. The need for improved catalysts formulations is evident.

7. Nomenclature

a	Yates–Satterfield reaction rate constant ($\mathrm{mol/kg_{cat}\,bar\,s}$)
a^*	Yates–Satterfield reaction rate constant ($\mathrm{m^6/mol\,kg_{cat}\,s}$)
A	reactor section ($\mathrm{m^2}$)
b	Yates–Satterfield absorption constant ($\mathrm{bar^{-1}}$)
b^*	Yates–Satterfield absorption constant ($\mathrm{m^3/mol}$)
$c_{G,CO}$	CO molar concentration in the gas phase ($\mathrm{mol/m^3}$)
c_{G,H_2}	H_2 molar concentration in the gas phase ($\mathrm{mol/m^3}$)
$c_{L,CO}$	CO molar concentration in the liquid phase ($\mathrm{mol/m^3}$)
c_{L,H_2}	H_2 molar concentration in the gas phase ($\mathrm{mol/m^3}$)
d_p	particle size (μm)
d_t	cooling tube diameter (mm)
D_L	diffusion coefficient in the liquid phase ($\mathrm{m^2/s}$)
$D_{L,ref}$	reference diffusion coefficient in the liquid ($\mathrm{m^2/s}$)
D_T	column diameter (m)
Fr	Froude number (dimensionless)
H	dispersion height of the reactor (m)
H_t	height of cooling tube (m)
k	Post reaction rate constant ($\mathrm{m^3/m^3_{cat}\,s}$)
k_La	volumetric mass transfer coefficient ($\mathrm{s^{-1}}$)
m_{CO}	Henry constant for CO (dimensionless)

m_{H_2}	Henry constant for H_2 (dimensionless)
P	total pressure (bar)
p_{CO}	CO partial pressure (bar)
p_{H_2}	H_2 partial pressure (bar)
Pr	Prandtl number (dimensionless)
R_{CO}	CO consumption rate ($mol/kg_{cat}\,s$)
R_{H_2}	H_2 consumption rate ($mol/kg_{cat}\,s$)
R_{CO+H_2}	synthesis gas consumption rate ($mol/kg_{cat}\,s$)
Re	Reynolds number (dimensionless)
St	Stanton number (dimensionless)
T	reactor temperature (K)
U_L	superficial liquid velocity (m/s)
U	superficial gas velocity (m/s)
$(U-U_{df})$	superficial gas velocity through the large bubbles (m/s)
U_{df}	superficial velocity of gas through the small bubbles (m/s)
V_o	pore volume of particles (m^3/kg)
V_{small}	rise velocity of the small bubbles (m/s)
$V_{small,ref}$	rise velocity of the small bubbles at 0% solids concentration (m/s)
z	axial coordinate (m)

Greeks

α	contraction factor (dimensionless)
α_{ASF}	Anderson-Schulz-Flory coefficient (dimensionless)
χ_{CO}	CO conversion (dimensionless)
χ_H	H_2 conversion (dimensionless)
χ_{CO+H2}	syngas conversion (dimensionless)
ϵ	total gas holdup (dimensionless)
ϵ_b	gas holdup referred to large bubbles (dimensionless)
ϵ_{df}	gas holdup referred to small bubbles (dimensionless)
$\epsilon_{df,ref}$	gas holdup referred to small bubbles at atmospheric conditions and 0% solids concentration (dimensionless)
ϵ_L	liquid phase holdup (dimensionless)
ϵ_s	solid volumetric concentration in the slurry phase (dimensionless)
μ_L	liquid viscosity (Pa s)
μ_{SL}	slurry viscosity (Pa s)
ρ_G	density of gas phase (kg/m^3)
$\rho_{G,ref}$	density of gas phase at atmospheric conditions (kg/m^3)
ρ_L	liquid density (kg/m^3)
ρ_p	particle density ($kg/m^3_{particle}$)
ρ_{SK}	solid skeleton density, (kg/m^3_{solids})
ρ_{SL}	slurry density, (kg/m^3_{slurry})

Subscripts

b	referring to large bubbles phase
CO	referring to CO species
df	referring to small bubbles
G	referring to gas phase
H_2	referring to H_2 species
L	referring to liquid phase
large	referring to large bubbles
p	referring to solid particle
s	referring to solids
SK	referring to solids skeleton
SL	referring to slurry
small	referring to small bubbles
trans	referring to regime transition point

Superscripts

i	referring to reactor inlet conditions
o	referring to reactor outlet conditions
*	referring to equilibrium conditions

References

[1] J.W.A. De Swart, R. Krishna, S.T. Sie, Proceedings of the Fourth International Natural Gas Conversion Symposium, Kruger Park, South Africa, 19–23 November 1995.
[2] B. Jager, Proceedings of the Fourth International Natural Gas Conversion Symposium, Kruger Park, South Africa, 19–23 November 1995.
[3] R. Krishna, J. Ellenberger, S.T. Sie, Chem. Eng. Sci. 51 (1996) 2041.
[4] R. Krishna, J. Ellenberger, AIChE J. 42 (1996) 2627.
[5] R. Krishna, J.W.A. de Swart, J. Ellenberger, G.B. Martina, C. Maretto, AIChE J. 43 (1997) 311–316.
[6] H.M. Letzel, J.C. Schouten, C.M. van den Bleek, R. Krishna, Chem. Eng. Sci. 52 (1997) 3733.
[7] J.W.A. de Swart, R.E. van Vliet, R. Krishna, Chem. Eng. Sci. 51 (1996) 4619.
[8] I.C. Yates, C.N. Satterfield, Energy Fuels 5 (1991) 168–173.
[9] M.F.M. Post, A.C. van't Hoog, J.K. Minderhoud, S.T. Sie, AIChE J. 35 (1989) 1107–1114.

[10] P.L. Mills, J.R. Turner, P.A. Ramachandran, M.P. Dudukovic, in: D.P. Nigam, A. Schumpe (Eds.), Three-Phase Sparged Reactors, Gordon and Breach, London, 1996.
[11] I.C. Yates, C.C. Chanenchuk, C.N. Satterfield, DOE Report no. PC79816-6, Contract no. DE-AC22-87PC79816, July–September 1989.
[12] I.G. Reilly, D.S. Scott, T.J.W. De Bruijn, D. Mac Intyre, Can. J. Chem. Eng. 72 (1994) 3–12.
[13] K. Akita, F. Yoshida, Ind. Eng. Chem. Process Des. Dev. 12 (1973) 76–80.
[14] P.M. Calderbank, M.B. Moo-Young, Chem. Eng. Sci. 16 (1961) 39.
[15] D.J. Vermeer, R. Krishna, Ind. Eng. Chem. Process Des. Dev. 20 (1981) 475–482.
[16] W.D. Deckwer, Y. Serpemen, M. Ralek, B. Schmidt, Ind. Eng. Chem. Process. Des. Dev. 21 (1982) 231–241.